TECHNICAL NOTE

EXPERIMENTAL AND NUMERICAL STUDY OF THE EFFECT OF A PIER ON SHIP TRAJECTORIES IN CURRENTS

(DOI No: 10.3940/rina.ijme.2014.a1.271tn)

W L Luo & C Guedes Soares Centre for Marine Technology and Engineering (CENTEC), Instituto Superior Técnico, University of Lisbon, Portugal, **Z J Zou** School of Naval Architecture, Ocean and Civil Engineering, Shanghai Jiao Tong University, Shanghai, China

SUMMARY

A study is presented of the effect of a pier on ship trajectories in currents. The current flow field around the pier is investigated. Experiments on ship manoeuvring and drift motion in the vicinity of a rectangular pier were carried out in a tank. Different current velocities and current angles were taken into account. The characteristics of the deviations of the ship trajectories from the initial course around the pier are investigated. Experimental findings indicate that the minimum required distance for safety navigation becomes larger with an increase of the current velocity. To obtain the details of continuous three-dimensional flow field around a pier, numerical simulation based on CFD calculations is conducted. The validity of the numerical simulation is demonstrated by comparison with experimental results.

1. INTRODUCTION

During last decades, research on ship collisions with bridges has been on-going continuously. In recent years more and more bridges over estuaries or rivers have been constructed, which raises the probability of ship collision with bridges, especially with the increasing waterborne traffic and large-scale ships. People are attaching more and more importance to such issue with the increase of safety and environmental consciousness. Since 1991, the American Association of State Highway and Transportation Officials (AASHTO) has promulgated the Guide Specification and Commentary for Vessel Collision Design of Highway Bridges [1], and the Load and Resistance Factor Design (LRFD) Bridge Design Specification [2]. The International Association for Bridge and Structural Engineering published a state-of-the-art report on Ship Collision with Bridges [3]. The Working Group 19 of the Inland Navigation Commission in the International Navigation Association reported the guidance for preventing ship-bridge collisions [4].

To guarantee the ship navigation safety and that of the bridge, it is necessary to study the mechanism of ship-bridge collision and to develop the measures of collision avoidance. The interaction between ship and pier is a special case of ship interaction with obstacles, which refer to the other ships, the banks and the offshore platforms. Many analytical and experimental studies on the general interaction have been presented. For example, the impact mechanics of ship-ship, ship-bank and ship-platform collisions were studied by analytical and close-form solutions [5]. The theoretical studies on hydrodynamic interactions between ships were performed with assumptions of ideal fluid and no free-surface effects [6]. The interaction between tug and ship was investigated by means of model measurements [7]. The slender-body theory was used to calculate the interactions of ships with fixed obstacles with the assumption of rigid free surface [8]. An empirical method was proposed for calculating the ship-bank interaction in restricted waters [9]. The Chimera RANS method was proposed for ship-ship interactions in shallow water and restricted waterway [10]. Experimental investigation was conducted on ship-bank interaction forces [11] and a new generic mathematical model to predict the ship-ship interaction forces was proposed [12]. The double-body potential-flow estimation was proposed for calculating the interaction forces between manoeuvring ships [13] and was validated in [14]. Piers are special obstacles and although many approaches did not study piers, actually they can be used for the research on ship-pier collision. For example, potential flow theories, including slender body theory and the method of non-uniform rational B-spline (NURBS), were proposed to calculate the interaction forces between ship and pier [15, 16].

For a long time, the efforts into ship-bridge collision have been mainly devoted to the determination of the impact force which is an important characteristic of ship-bridge collision. The determination of impact force has been developed from general formulas for equivalent loads, based on collision tests, to numerical simulations [17]. To predict the ship-bridge collisions, the approaches based on probabilistic risk assessment (PRA) are in common use [18-20]. To obtain a probability based model, it is usually required to investigate the vessel traffic under a bridge and to collect the accident data of ship-bridge collisions. Because the ship-bridge collision is a small probability event, it is difficult to acquire enough statistical samples and consequently the validity of PRA based method has certain limitations in application.

When collision happens, the impact force depends on the impact velocity and direction. These two variables are determined by many factors including the velocity and

heading angle of a ship at the time of deviating from initial course, distance between the ship and bridge, inherent manoeuvrability of the ship, interaction between the ship and pile, and the environmental disturbances such as wind, wave and current. Therefore, from the viewpoint of active protection of bridge against ship collision, not only the dynamical responses of bridge and pier, but also characteristics of ship motion should be focused on. Despite the fact current researches on ship-bridge collision care less about the characteristics of ship motion, some experimental and calculation results have been presented. Experiments in a water tank with wind capabilities were conducted to analyse the effect of wind on the course-keeping of a ship in the vicinity of a pier [21]. Presented were analytical and experimental studies on the ship manoeuvring behaviours subjected to a sheering flow induced around a pier [22]. Calculations were made with the application of the aforementioned potential flow theory [15,16], and with analytical and simulation methods for determining vessel's safety manoeuvring area [23]. Although some literature has presented the numerical simulations of the flow field around a pier, e.g. in [24, 25], little attention was paid to the effect of the flow field on ship navigation.

This paper presents a preliminary study of the effect of a pier on ship trajectories in currents. Experiments of ship manoeuvring and drift motion in the vicinity of a rectangular pier were carried out considering different current speeds and directions. The characteristics of the deviation of ship trajectories from the initial course in the vicinity of the pier are investigated. A Computational Fluid Dynamics (CFD) model is used to calculate the three-dimensional flow field around a pier. Standard k-ε turbulent model and the finite volume method (FVM) is adopted in the calculation. The validity of numerical simulation is verified in comparison with the experimental results.

2. EXPERIMENTS ON SHIP TRAJECTORIES IN THE VICINITY OF A PIER

Free-running model tests were carried out in a wind wave current (WWC) tank with the dimension $90\text{m}\times15\text{m}\times2\text{m}$ (length×width×depth), in Shanghai Ship and Shipping Research Institute (SSSRI), China. The depth of water is adjustable. The ship model is a type of container ship with a six-tier-height superstructure. The steering equipment includes a propeller and a rudder fixed in the middle of stern, as shown in Figure 1. The main particulars of the ship model and appendages are given in Table 1.

A pier model was made with the rectangular profile shown in Figure 2, in which the ratio of the lateral length of pier to its longitudinal length is $B_P / L_P = 0.5$ and the origin of earth-fixed coordinate system is selected as the centre of the pier. The x_0-coordinate directs to the true north. The depth of water was adjusted to 0.6m and the pier crossed the free surface vertically. Since the focus in this research is on the effect on ship motion, caused by current around a pier instead of by bridge, not any load exerted on the pier from above was presumed. The pier was fixed centrally at the bottom of the tank during experiments.

Table 1. Principal particulars of the ship model and appendages

Item	Model	Item	Rudder	Item	Propeller
Scale ratio	1:100	Type	streamline	Diameter	65mm
L_{oa}	2.7 m	Height	11.8cm	Pitch ratio	1.2
L_{pp}	2.55 m	Aspect ratio	1.628	Number of blades	5
Breadth(B)	0.42 m			Area ratio	1.0
Ship depth(D)	0.224 m			Rake angle	8°
Draft(T)	0.15 m				

Figure 1- Ship model, propeller and rudder

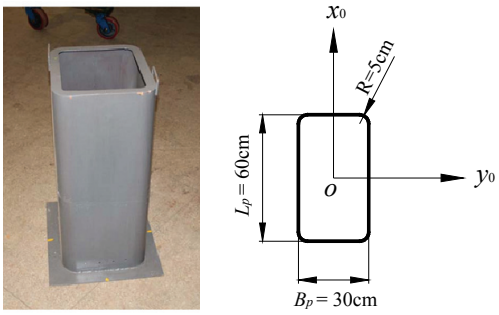

Figure 2- Pier model

2.1 EXPERIMENTAL SET UP

In the experiments, the ship model passed by the pier in currents with steering and without steering respectively. Current speeds were designed as 0.1m/s and 0.2m/s, with current angles 0°, 5°, and 10° respectively. All currents generated direct from north to south. Note that because the current generating system is unmovable, to obtain

different current angles, the pier had to be rotated to the desired orientation if the current angle was nonzero.
When the ship was under control, the revolutions of propeller remained unchanged following the calibration tests of ship velocity, in which the model ship was required to sail at a nominal speed V = 0.6m/s with reference to the bank. Moreover, the heading angles were requested to be zero by adjusting the rudder angles, which means that the longitudinal line of ship was requested to be parallel to the x_0-directional centreline of the pier, as shown in Figure 3, in which ψ_c is the current angle by positive definition of clockwise rotation from x_0-coordinate.

In the event of out-of-control, the ship moved straight from the start at a demanded speed before it reached a predetermined position. Afterwards, the steering engine and the motor in propeller were shut down. When the ship was in lost control mode, she began moving freely from the spots 2.5m and 5m longitudinally away from the pier respectively. Whether the free ship could safely pass by the pier under the actions of inertia and hydrodynamic forces is the concern of the experiment. To understand how far the pier affected the ship motion, the lateral offsets between the desired trajectories and the centreline of the pier were designed to be 0.5m and 1.0m respectively, as shown in Figure 3.

In experiments, the time histories of the trajectories of the gravity centre of ship, the ship velocities, heading angles, and rudder angles were recorded.

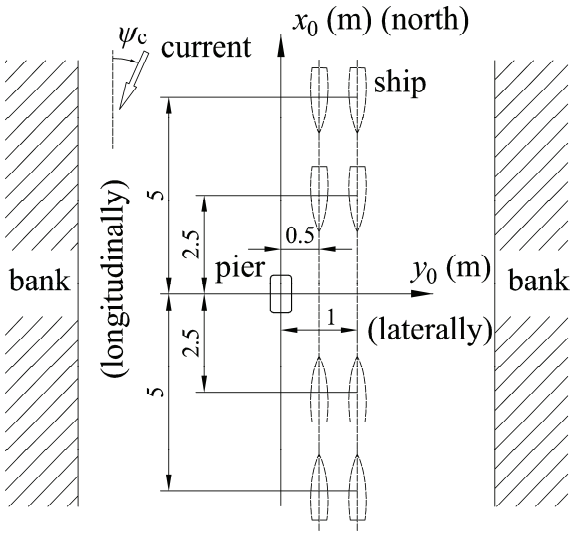

Figure 3- Manoeuvring tests in current

2.2 EXPERIMENTAL RESULTS AND ANALYSIS

In the experiments, some of the test runs started from upstream (north) to downstream (south) while the rest of runs pointed the opposite direction. Generally, it is easier to control the ship moving upstream than downstream, which was confirmed by the actual ship steering experiences. To investigate the required safety distance of the ship from the pier, the sway displacements of ship are studied. By analysis of the test results, it is concluded that the minimum lateral distance of the ship course from the pier centreline ($y_0 = 0.5$m) satisfies the requirement of safety navigation, even with the maximum current velocity ($V_C = 0.2$m/s) and maximum current angle (ψ_c =10°), with or without steering. To illustrate it, examples are presented in Figure 4 and Figure 5-10.

Figure 4 shows an example of the normalized maximum sway deviations $\Delta y_{\max} / L_S$ from the desired ship straight courses with respect to the normalized coordinate of desired ship course y_0 / B_P, with steering and in the cases of different current speeds and orientations. Herein, L_S is the overall ship length, i.e. L_{oa}; V_C is the current velocity and V_S the ship velocity.

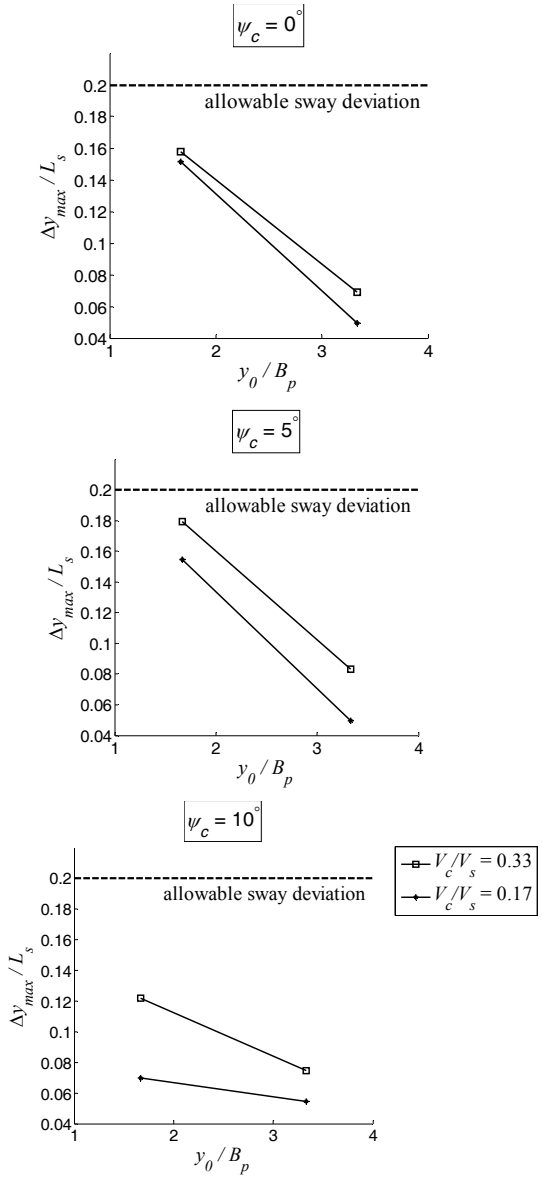

Figure 4 - Relationship between the normalized maximal sway deviation and the normalized coordinate of desired ship course

It can be seen in Figure 4 that the maximum sway deviation becomes larger with a decrease of distance between the pier and the ship trajectory, and with an increase of current velocity. It is indicated that the minimum required distance for safety navigation or collision avoidance becomes larger with an increase in the velocity of tidal currents relative to the ship velocity. Unfortunately, due to the experimental limitations, no minimum required safety distance of the ship course from the pier centre is obtained from Figure 4. This index could have been achieved provided with a more comprehensive test programme. Supposing that the allowable sway deviation from the desired course is limited to 0.2 times the ship length from the viewpoint of safe ship handling or ship-pier collision avoidance, which was recommended in [22], as can be seen from Figure 4, the maximum current velocity $V_C / V_S = 0.33$, the maximum current angle ψ_c =10°, and the minimum lateral distance of ship course from the pier centreline $y_0 / B_P = 1.67$, satisfy the requirement of safe navigation.

Table 2. Average sway deviations ($\overline{\Delta y} / L_S$), V_c /V_c = 0.33, $\psi_c = 0°$

Offset (y_0 / B_P)	Average sway deviation (upstream)	Average sway deviation (downstream)
1.67	0.026	0.028
3.34	0.027	0.056

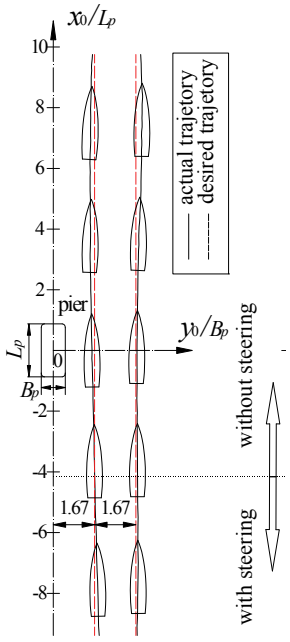

Figure 5- Examples of ship trajectories for out-of-control ship (upstream, $V_C / V_S = 0.33$,$\psi_c = 0°$)

Figures 5-10 show the examples of the histories of ship trajectories for a lost ship with current speed $V_C / V_S = 0.33$ and orientation ψ_c = 0°, 5°, 10° respectively. The average sway deviations $\overline{\Delta y} / L_S$ from the desired ship straight courses are listed in Tables 2 to 4. In Figure 5, 7 and 9, the ship model is travelling upstream. In Figure 6, 8 and 10, it is travelling downstream. When the ship is out of control, it moves freely from the location 2.5m longitudinally from the pier.

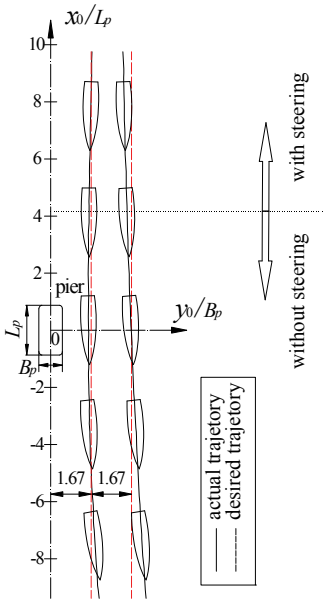

Figure 6- Examples of ship trajectories for out-of-control ship (downstream, $V_C / V_S = 0.33$,$\psi_c = 0°$)

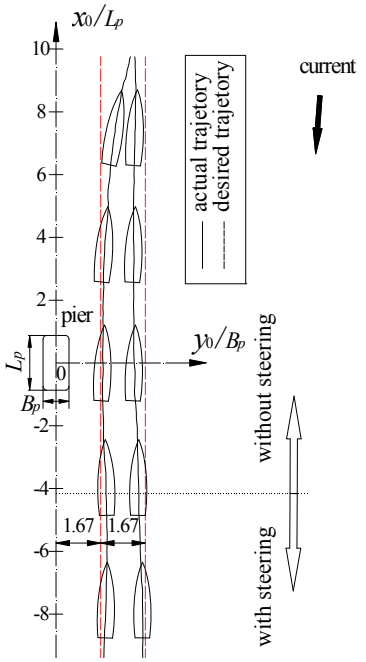

Figure 7- Examples of ship trajectories for out-of-control ship (upstream, $V_C / V_S = 0.33$,$\psi_c = 5°$)

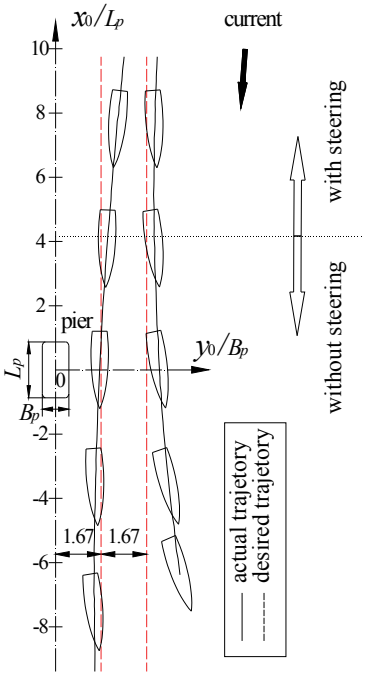

Figure 8- Examples of ship trajectories for out-of-control ship (downstream, $V_C / V_S = 0.33$,$\psi_c = 5°$)

Table 3. Average sway deviations ($\overline{\Delta y} / L_S$), V_c /V_c = 0.33, $\psi_c = 5°$

Offset (y_0 / B_P)	Average sway deviation (upstream)	Average sway deviation (downstream)
1.67	0.074	0.077
3.34	0.072	0.116

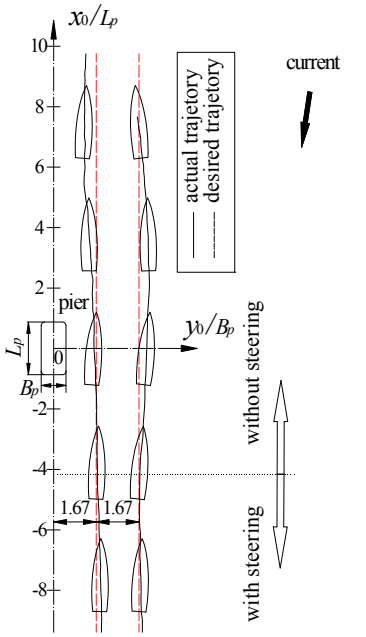

Figure 9- Examples of ship trajectories for out-of-control ship (upstream, $V_C / V_S = 0.33$,$\psi_c = 10°$)

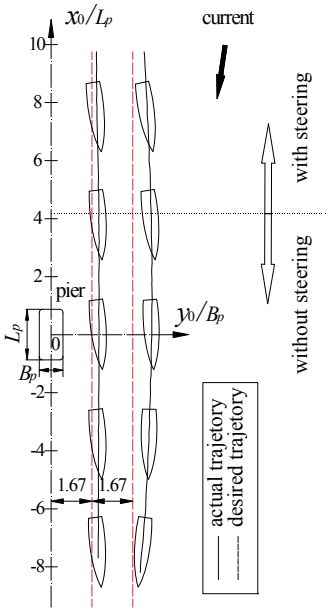

Figure 10- Examples of ship trajectories for out-of-control ship (downstream, $V_C / V_S = 0.33$,$\psi_c = 10°$)

As can be seen from the experimental results, little influence of the flow field around the pier is exerted on the ship course keeping, both in the case of 0.5m lateral offset ($y_0 / B_P = 1.67$) and 1m lateral offset ($y_0 / B_P = 3.34$) from the pier. It can also be seen that, for a ship travelling downstream, the deviation from the desired course is more severe than the upstream case.

Table 4. Average sway deviations ($\overline{\Delta y} / L_S$), V_c /V_c = 0.33, $\psi_c = 10°$

Offset (y_0 / B_P)	Average sway deviation (upstream)	Average sway deviation (downstream)
1.67	0.052	0.058
3.34	0.041	0.132

The above conclusion can be validated by individual tests in current, which aimed to assist in the analysis of the effect of the pier on the ambient flow field. In such tests, current speeds were measured 5cm below the water surface by a flow meter at eleven different locations, as shown in Figure 11. The current generated directed from north to south. The measurement spots A_0, A_1, A_2, and A_3 were distributed upstream; B_1, B_2, and B_3 were located at the transversal centreline of the pier; C_0, C_1, C_2, and C_3 were located downstream. The lateral offsets between the centreline of pier and the measuring points were selected as 0.5m, 1.0m, and 1.5m while the longitudinal offset was selected as 1m for points A_i and C_i (i=0,1,2,3).

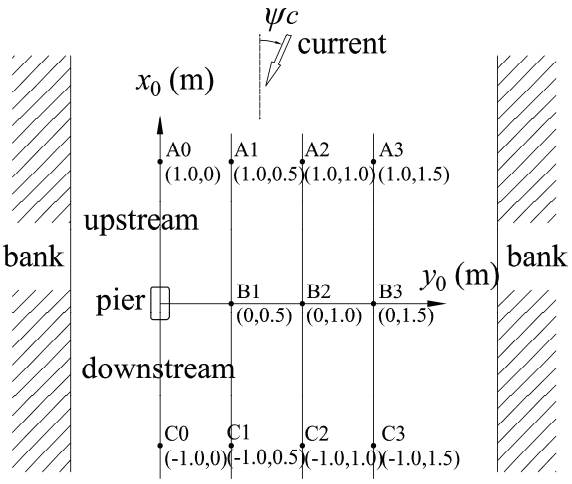

Figure 11- Distribution of measuring points w.r.t. current speeds

The test results are given from Table 5 to Table 10. Note that the unit of the current velocity in model tests is cm/s, instead of the presented unit m/s. As can be seen from the results, in the direction perpendicular to the current and outside the spots 0.5m away from the pier, current is less affected by the pier. By contrast, the test results of points A_0 and C_0 indicate that the pier makes an obvious effect on the current in the right upstream and downstream regions, especially for the right downstream region, which will be confirmed by forthcoming CFD calculation. It should be noted that measurements of current in line with the pier (x_o-direction) are only provided for the cases of $\psi_c = 0°$, shown in Tables 5 and 6. As aforementioned, when the current direction is nonzero, the pier is rotated to the desired orientation because the current generating system is unmovable. Therefore, in Tables 7 to 10, the measurements of current at locations A_0 and C_0 for the cases of $\psi_c = 5°$ and $\psi_c = 10°$ are not provided.

Table 5. Current speeds (m/s), nominal speed V_d =0.1m/s, $\psi_c = 0°$

Location	V_c	Location	V_c	Location	V_c
A0	0.0882			C0	0.0606
A1	0.0948	B1	0.0972	C1	0.0957
A2	0.0986	B2	0.0995	C2	0.1001
A3	0.0974	B3	0.0967	C3	0.0985

Table 6. Current speeds (m/s), nominal speed V_d =0.2m/s, $\psi_c = 0°$

Location	V_c	Location	V_c	Location	V_c
A0	0.1782			C0	0.1273
A1	0.1776	B1	0.1795	C1	0.1752
A2	0.1862	B2	0.1891	C2	0.1881
A3	0.1881	B3	0.1915	C3	0.1905

Table 7. Current speeds (m/s), nominal speed V_d =0.1m/s, $\psi_c = 5°$

Location	V_c	Location	V_c	Location	V_c
A1	0.0999	B1	0.1054	C1	0.1034
A2	0.104	B2	0.1064	C2	0.1026
A3	0.1046	B3	0.1042	C3	0.1083

Table 8. Current speeds (m/s), nominal speed V_d =0.2m/s, $\psi_c = 5°$

Location	V_c	Location	V_c	Location	V_c
A1	0.1852	B1	0.1990	C1	0.1972
A2	0.1958	B2	0.1884	C2	0.1932
A3	0.1972	B3	0.2009	C3	0.2021

Table 9. Current speeds (m/s), nominal speed V_d =0.1m/s, $\psi_c = 10°$

Location	V_c	Location	V_c	Location	V_c
A1	0.1016	B1	0.1101	C1	0.1103
A2	0.0999	B2	0.0997	C2	0.102
A3	0.0984	B3	0.1003	C3	0.1023

Table 10. Current speeds (m/s), nominal speed V_d =0.2m/s, $\psi_c = 10°$

Location	V_c	Location	V_c	Location	V_c
A1	0.1950	B1	0.2048	C1	0.1941
A2	0.1948	B2	0.1931	C2	0.1918
A3	0.1949	B3	0.2005	C3	0.2012

Note that there are some inevitable system errors in the tests, which results in the deviation of actual current speed from the desired current speed even when the current is not affected by the pier. Such errors are mainly caused by the measuring instruments, however allowable by error analysis.

3. NUMERICAL SIMULATIONS

Although the experimental method is regarded as the most credible approach in many scientific research fields, some limitations hinder its popular use. The main obstacle is the experimental expense that many colleges or institutes cannot afford. Analytical investigation is an alternative; however it is known that in most cases, to obtain precise analytical solutions is challenging. Another significant challenge is the availability of reliable and well documented experimental data for the purposes of validating numerical techniques. As for the study on ship-bridge collision, few theoretical investigations are available in literature except for those by Minorsky [26] and by Iwai [22]. With the development of computer technology, numerical simulation methods have found wider applications and have been proven a powerful solution tool in many engineering areas, e.g. in the field of ship and ocean engineering.

In this paper, the CFD technique is used to calculate the three-dimensional flow field around a pier. As a preliminary study, no free surface and ship motion are taken into account. Only the modelling of the current flow field around the pier is focused on. The future work will extend the numerical study to include the modelling of the ship's trajectory.

Because the influence of pier on the flow field is restricted to a limited area, the calculation domain is set as a cuboid with $45\text{m} \times 7.5\text{m} \times 0.6\text{m}$ so as to reduce the calculation time, as shown in Figure 12.

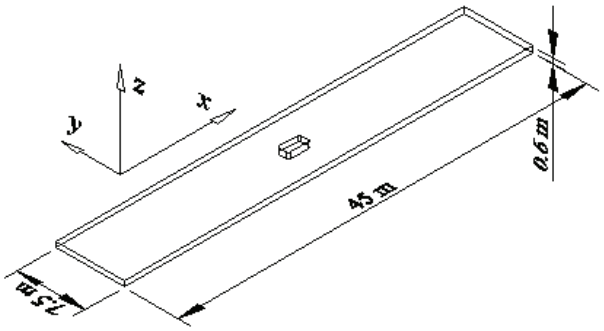

Figure 12- Calculation model

In mesh generation, refinement is conducted along the profile of the rectangular pier, shown as Figure 13.

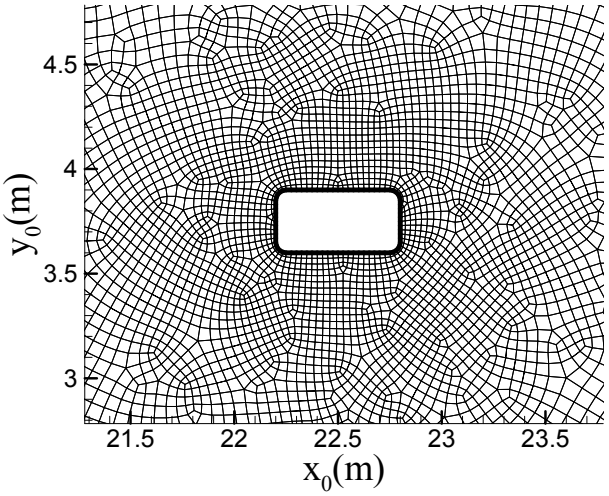

Figure 13- Mesh adopted for the calculations

Taking the minimum current speed (0.1m/s) and minimum current angle (0°) as an example, and also the pier's width as the characteristic length, the Reynolds number can be calculated as $R_e \approx 0.3 \times 10^5$. Therefore, the Reynolds-Averaged Navier-Stokes (RANS) equations are applied, in which the standard k-ε turbulent mode is adopted.

3.1 THE GOVERNING EQUATIONS

The continuity equation is

$$\frac{\partial U_i}{\partial X_i} = 0, \tag{1}$$

where U_i is the flow velocity in X_i direction.

The momentum equation is

$$\frac{\partial(\rho U_i)}{\partial t} + \frac{\partial(\rho U_j U_i)}{\partial X_j} = -\frac{\partial P}{\partial X_i} + \frac{\partial}{\partial X_j}\left((\mu + \mu_t)\left(\frac{\partial U_i}{\partial X_j} + \frac{\partial U_j}{\partial X_i}\right)\right), \tag{2}$$

where ρ is the density of flow; P the pressure; μ and μ_t are respectively the dynamic viscosity of flow and turbulent viscosity which is determined by turbulent kinetic energy k, model constant C_μ, and dissipation ε,

$$\mu_t = \rho C_\mu \frac{k^2}{\varepsilon}. \tag{3}$$

The transport equations are as follows. For turbulent kinetic energy k, it holds that

$$\frac{\partial(\rho k)}{\partial t} + \frac{\partial(\rho U_j k)}{\partial X_i} = \frac{\partial}{\partial X_i}\left(\left(\mu + \frac{\mu_t}{\sigma_k}\right)\frac{\partial k}{\partial X_i}\right) + G - \rho\varepsilon, \tag{4}$$

where σ_k is the model constant; G the production of turbulent kinetic energy,

$$G = \mu_t\left(\frac{\partial U_i}{\partial X_j} + \frac{\partial U_j}{\partial X_i}\right)\frac{\partial U_i}{\partial X_j}. \tag{5}$$

For dissipation ε, one has

$$\frac{\partial(\rho\varepsilon)}{\partial t} + \frac{\partial(\rho U_j \varepsilon)}{\partial X_i} = \frac{\partial}{\partial X_i}\left(\left(\mu + \frac{\mu_t}{\sigma_\varepsilon}\right)\frac{\partial \varepsilon}{\partial X_i}\right) + C_{1\varepsilon} G \frac{\varepsilon}{k} - C_{2\varepsilon}\rho\frac{\varepsilon^2}{k}, \tag{6}$$

where σ_ε, $C_{1\varepsilon}$ and $C_{2\varepsilon}$ are model constants.

3.2 CALCULATION RESULTS AND ANALYSIS

Calculations are performed by using FLUENT commercial software. The finite volume method (FVM) is adopted to represent and evaluate the above partial differential equations. Figure 14 shows the calculated distribution of flow field in the vicinity of the pier, on a plane with 0.55m water depth away from the bottom of tank. Three current angles, 0°, 5°, 10°, and two inlet velocities, 0.1m/s, 0.2m/s, are taken into account.

The left part of Figure 14 presents the contours of current velocity magnitude around the pier and the right plot shows the streamlines. It can be seen from the figure that, as the streamlines approach the pier from upstream, part of them flow directly to the pier and slow down when arriving at the pier, while other pass by the pier and reach the maximum velocities at the two ends along the pier width. Behind and near the pier, trailing vortices form due to the separation of boundary layers and the current velocities decrease. These observations are consistent with experimental or numerical analyses in the literatures, e.g. in [27, 28].

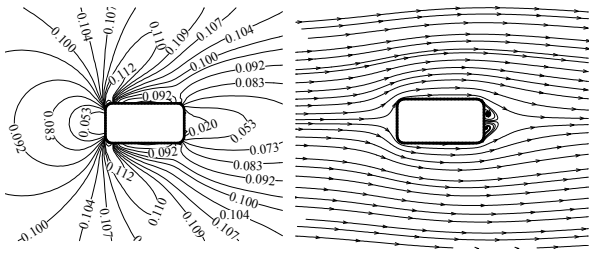

Figure 14(a)- Distribution of flow field around a pier with $\psi_c = 0°$ and inlet velocity = 0.1m/s

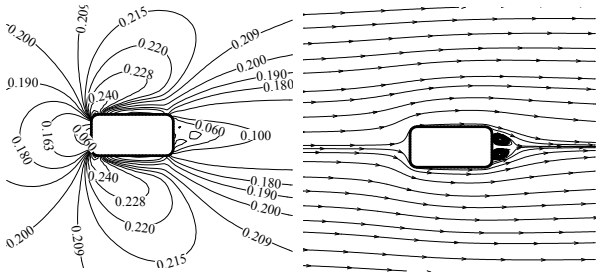

Figure 14(b)- Distribution of flow field around a pier with $\psi_c = 0°$ and inlet velocity = 0.2m/s

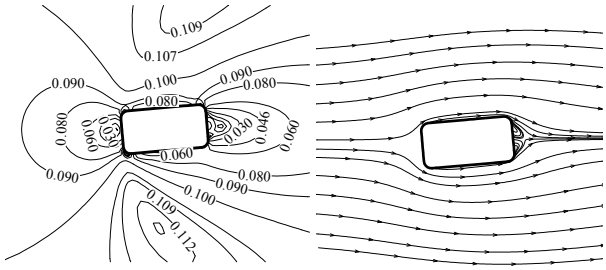

Figure 14(c)- Distribution of flow field around a pier with $\psi_c = 5°$ and inlet velocity = 0.1m/s

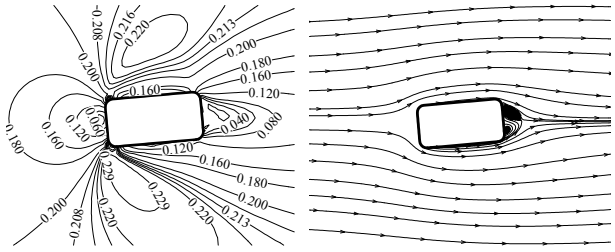

Figure 14(d)- Distribution of flow field around a pier with $\psi_c = 5°$ and inlet velocity = 0.2m/s

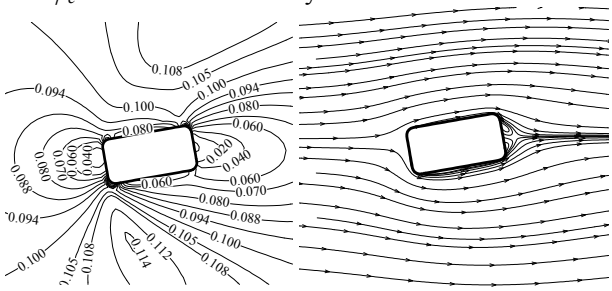

Figure 14(e)- Distribution of flow field around a pier with $\psi_c = 10°$ and inlet velocity = 0.1m/s

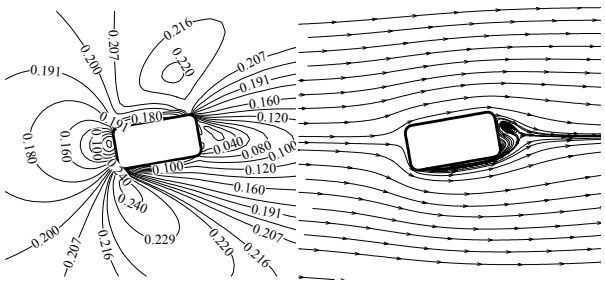

Figure 14(f)- Distribution of flow field around a pier with $\psi_c = 10°$ and inlet velocity = 0.2m/s

To verify the validity of CFD calculation, comparisons are conducted between the results of numerical simulation and those from experiments on current speeds.

Figure 15 presents the comparison of current speeds between CFD calculation and experiments at the eleven locations in Figure 11. It can be seen from the figure that, the calculation results mostly agree with the experiments. The average relative error of CFD calculations is 6.7%. The largest difference occurs at the point B_1 with 0.2m/s current speed and 0° current angle. The second largest difference refers to the point C_1 with 0.1m/s current speed and 10° current angle.

At the point B_1, the numerical simulation result is obviously larger than that of experiment, larger than nominal current speed (0.2m/s) as well.

It is confirmed that streamlines passing by a pier reach the maximum velocities at two ends of the pier along the pier's width. Furthermore, because the variation of current speed is continuous, in some area on either side of the pier, the current velocities are larger than the nominal current speed. Far away from the pier, there is little change with current speed. Therefore, it is concluded that the error at B_1 results mainly from measurements.

At the point C_1, the numerical simulation result is obviously smaller than that of the experiment, also smaller than the nominal current speed (0.1m/s). As aforementioned, in the rear of pier, a couple of trailing vortices come into being because of the effect of boundary layer. The dynamic pressures in the area of vortices become lower and correspondingly, the current speed behind a pier is smaller than the nominal one. Consequently, just like the error analysis for B_1, measurement accounts for the error at C_1. As a matter of fact that the measurement system error is inevitable; in a sense, the CFD technique is helpful for the modification and error analysis of experiment.

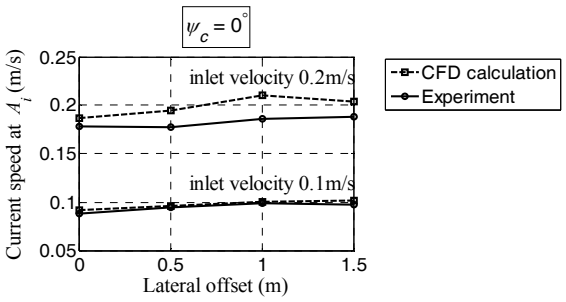

Figure 15(a)- Comparison of current speeds (upstream) between CFD calculation and experiments with $\psi_c = 0°$

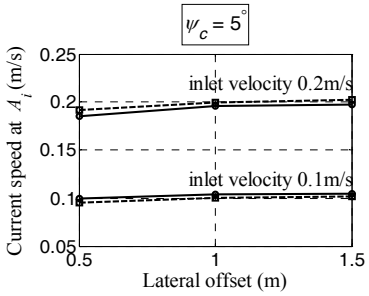

Figure 15(b)- Comparison of current speeds (upstream) between CFD calculation and experiments with $\psi_c = 5°$

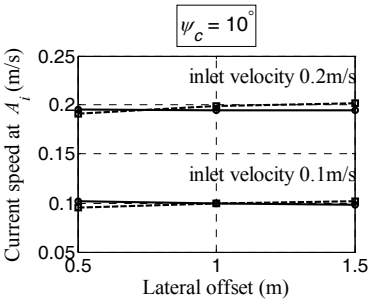

Figure 15(c)- Comparison of current speeds (upstream) between CFD calculation and experiments with $\psi_c = 10°$

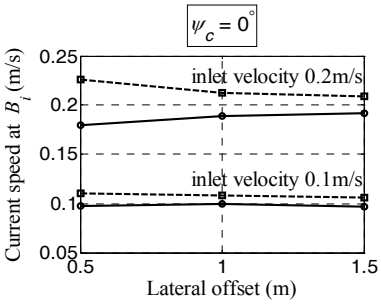

Figure 15(d)- Comparison of current speeds (midstream) between CFD calculation and experiments with $\psi_c = 0°$

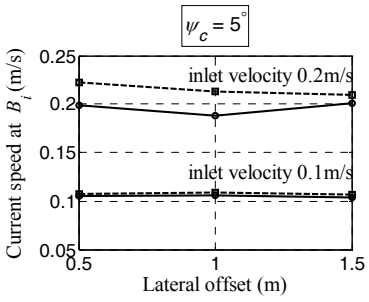

Figure 15(e)- Comparison of current speeds (midstream) between CFD calculation and experiments with $\psi_c = 5°$

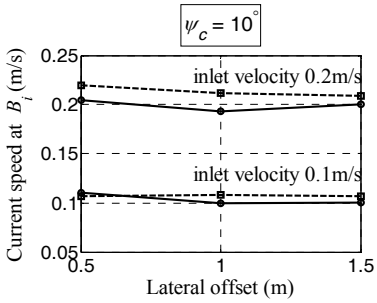

Figure 15(f)- Comparison of current speeds (midstream) between CFD calculation and experiments with $\psi_c = 10°$

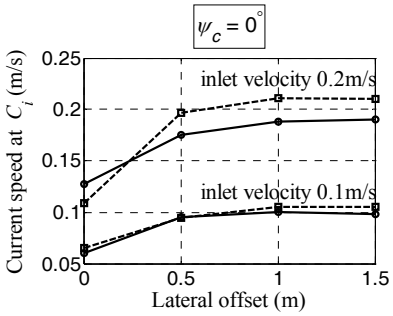

Figure 15(g)- Comparison of current speeds (downstream) between CFD calculation and experiments with $\psi_c = 0°$

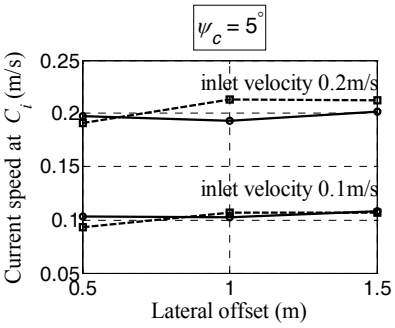

Figure 15(h)- Comparison of current speeds (downstream) between CFD calculation and experiments with $\psi_c = 5°$

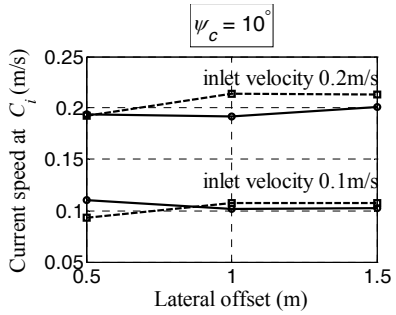

Figure 15(i)- Comparison of current speeds (downstream) between CFD calculation and experiments with $\psi_c = 10°$

To investigate the affected region of the pier, the variations of current speed laterally along the "channel" are also simulated. Figure 16 presents an example of variation with 0.1m/s current speed and 0° current angle, in which H=0.6m is the height of 'pier'. The results of the other cases are similar to the one presented.

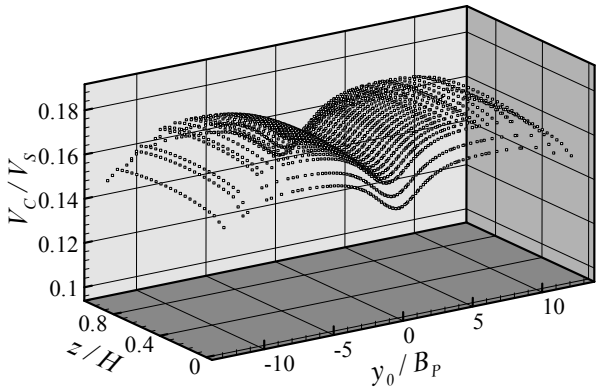

Figure 16(a)- scatter of current velocities 1m ahead of the pier, lateral variations of current speed in the vicinity of a pier with $\psi_c = 0°$ and inlet velocity = 0.1m/s

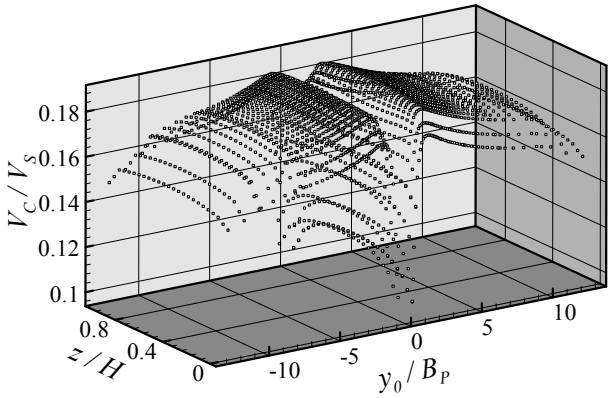

Figure 16(b)- scatter of current velocities along lateral the centreline of pier, lateral variations of current speed in the vicinity of a pier with $\psi_c = 0°$ and inlet velocity = 0.1m/s

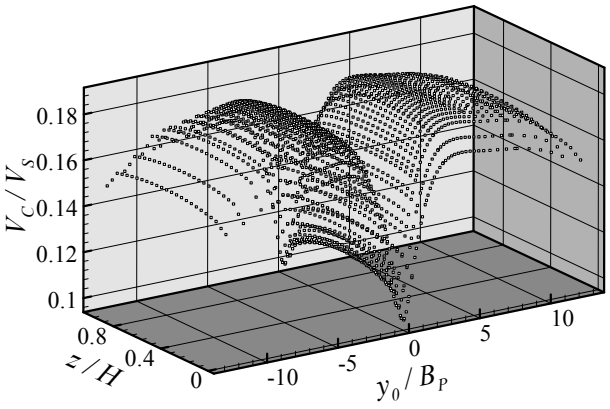

Figure 16(c)- scatter of current velocities 1m behind the pier, lateral variations of current speed in the vicinity of a pier with $\psi_c = 0°$ and inlet velocity = 0.1m/s

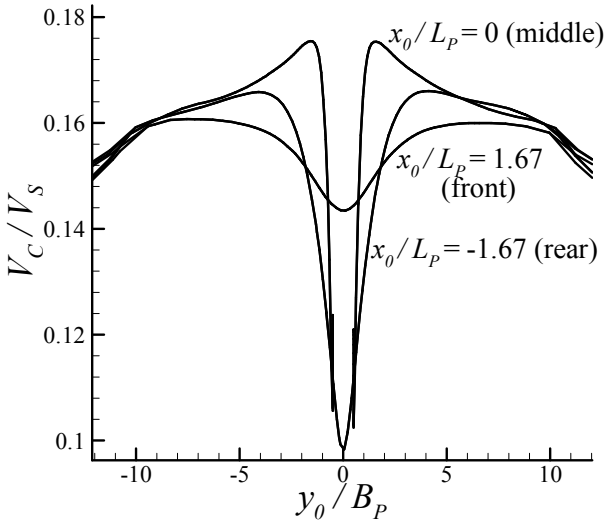

Figure 16(d)- comparison of three patterns on a plane near surface, lateral variations of current speed in the vicinity of a pier with $\psi_c = 0°$ and inlet velocity = 0.1m/s

As can be seen from Figure 16, the flow field far away from the pier is uniform; in the area right ahead of pier, the lateral variation of current speed is with small amplitude; on both sides and right behind the pier however, there are significant change with current speed, especially on the both sides of pier.

4. CONCLUSIONS

This paper presents the preliminarily experimental and numerical investigations into the flow field around a rectangular pier and its effect on ship trajectories. Experimental conditions address such factors as configuration of steering forces, environmental disturbances induced by current with different velocities

and directions, clearance distance between the ship and pier, and ship moving orientations.

Numerical simulations are conducted by using CFD calculation to obtain the three-dimensional flow field in the vicinity of a pier. Standard k-ε turbulent model is adopted in the calculations. Based on experimental and numerical analyses, some preliminary conclusions are made as follows.

Experimental results indicate that to control a ship moving upstream is easier than to control a ship moving downstream. Such findings support previous studies and the navigator's experience. For the sake of safe navigation, special attention should be paid to the ship handling when the ship moves downstream.

The maximum sway deviation of a ship becomes larger with a decrease of distance between pier and ship course, and with an increase of current velocity. Due to the experimental limitations, no minimum required safety distance of the ship course from the pier centre is obtained. It can be only said in this paper that the lateral distance of ship course from the pier centreline, 1.67 time the pier width ($1.67B_P$), and the current velocity, 0.33 time the ship velocity ($V_C / V_S = 0.33$), satisfy the requirement of safety navigation, no matter whether the ship is in steering or not.

The current flow field around a pier is investigated by experiments and CFD calculation. By observing the experimental results and CFD calculation results, it can be concluded that the pier exerts an influence on the ambient flow field. Near the pier, flow velocities decrease in the area right ahead of pier because of the blockage effect by pier; so do in the right rear of pier due to the trailing vortices. Especially, the velocity decrease downstream is more obvious. On both sides of the pier, except for the boundary layer, flow velocities become larger than inlet velocity. Comparatively, the pier affects less the flow right ahead of the pier. These variations of flow field have been confirmed either by experiments or CFD calculation.

Modelling of the current flow field around a pier is carried out by CFD. CFD based numerical simulations provide an effective way to obtain the continuous three-dimensional flow field around a pier. On the contrary, only discrete measurements can be obtained by experiments. CFD calculations can compensate the insufficiency of experimental method, and also can assist in the modification and error analysis of experiment. In this paper, the characteristics of the ambient flow field calculated by CFD are consistent with published analyses in literatures. Its validity is verified by comparison with experimental results.

Future work will be devoted to further numerical research on the ship manoeuvring and drift motion in the vicinity of a pier. As a preliminary study, neither free surface nor ship motion is considered in this paper for the calculation of the flow field around the pier. In the next work, not only the details of the flow field around the pier, but also the interaction between the pier and the ship, the ship manoeuvrability near the pier as well, will be focused on. By calculating or predicting the ship motions in the cases of a closer distance to the pier and more severe tidal current, the minimum distance of the ship course from the pier centre and the maximal current velocity can be determined and applied to the ship-pier collision avoidance.

5. ACKNOWLEDGEMENTS

This work was partially supported by the China Scholarship Council, and the Natural Science Foundation of Fujian Province of P.R. China (No. 2010J01004).

6. REFERENCES

1. THE AMERICAN ASSOCIATION OF STATE HIGHWAY AND TRANSPORTATION OFFICIALS (AASHTO), *Guide Specification and Commentary for Vessel Collision Design of Highway Bridges*, Second Edition, USA, 2009.
2. AASHTO, *AASHTO LRFD Bridge Design Specifications (5th Edition) with 2010 Interim Revisions*, USA, 2010.
3. LARSEN, O.D., Ship Collision with Bridges – The Interaction between Vessel Traffic and Bridge Structures. In: *Structural Engineering Documents 4*, International Association of Bridge and Structural Engineering (IABSE), Zurich, 1993.
4. PIANC-WG19 (Working Group 19 of the Inland Navigation Commission), Ship Collision Due to the Presence of Bridges. In: *PIANC Report of InCom WG 19*, International Navigation Association, Belgium, 2001.
5. PEDERSEN, P.T., On Impact Mechanics in Ship Collisions, *Marine Structures*, 11, pp. 429-449, 1998.
6. TUCK, E. O. AND NEWMAN, J. N., Hydrodynamic Interactions between Ships, *Proceedings of 10th Symposium on Naval Hydrodynamics*, June 24-28, 1974, Cambridge, MA, 35–69, 1974.
7. DAND, I.W., Some Aspects of Tug-ship Interaction, *Proceedings of 4th International Tug Convention*, New Orleans, LA, Paper No. 5: Thomas Reed Industrial Publications, London, UK, 61–80. 1975.
8. YEUNG, R.W. AND TAN, W.T., Hydrodynamic Interactions of Ships with Fixed Obstacles, *Journal of Ship Research*, 24, 50–59, 1980.
9. CH'NG, P. W., DOCTORS, L. J. AND RENILSON, M. R., A Method of Calculating

the Ship-Bank Interaction Forces and Moments in Restricted Water, *International Shipbuilding Progress*, 40, 421, 7–23, 1993.

10. CHEN H.-C., LIN W.-M. AND HWANG W.-Y., Validation and Application of Chimera RANS Method for Ship-ship Interactions in Shallow Water and Restricted Waterway, *Proceedings of 24th Symposium on Naval Hydrodynamics*, Fukuoka, Japan, July 2002.
11. VANTORRE, M., DELEFORTRIE, G., ELOOT, K. AND LAFORCE, E., Experimental investigation of ship-bank interaction forces, *Proceedings of International Conference on Marine Simulation and Ship Maneuverability*, August 25–28, Kanazawa, Japan, Vol. 3, RC-31-1–RC-31-9, 2003.
12. VARYANI, K. S., THAVALINGHAM, A. AND KRISHNANKUTTY, P., New Generic Mathematical Model to Predict Hydrodynamic Interaction Effects for Overtaking Manoeuvres in Simulators, *Journal of Marine Science and Technology*, 9, 24–31, 2004.
13. ZHOU, X.; SUTULO, S., AND GUEDES SOARES, C. 2010; Computation of Ship-to-Ship Interaction Forces by a 3D Potential Flow Panel Method in Finite Water Depth. Proceedings of the 29th International Conference on Ocean, Offshore and Arctic Engineering (OMAE 2010); Shanghai, China. ASME paper OMAE2010-20497.
14. SUTULO, S., GUEDES SOARES, C. AND OTZEN, J.F., Validation of potential-flow estimation of interaction forces acting upon ship hulls in side-to-side motion, *Journal of Ship Research*, 56, 3, 129-145, 2012.
15. KIJIMA, K., Prediction Method for Ship Manoeuvring Motion in the Proximity of a Pier, *Ship Technology Research*, 44 (1), pp.22-31, 1997.
16. ZHANG, X. T., TENG, B., LIU, Z. Y. AND ZHANG, L. W., Unsteady Computation of Hydrodynamic Interaction Forces and Moments between Ship Hull and Pier Based on NURBS, *Journal of Ship Mechanics*, 7(6), pp.47-53, 2003.
17. SVENSSON, H., Protection of Bridge Piers against Ship Collision, *Steel Construction*, 1, pp. 21-32, 2009.
18. KENNETH, B. B., *Structural Reliability Analysis for Vessel Impact on Bridges*, Master Degree Thesis, The University of Texas at Austin, USA, 2005.
19. DAVIDSON, M. T., *Probability Assessment of Bridge Collapse under Barge Collision*, Doctoral Dissertation, University of Florida, USA, 2010.
20. LIM, J.-H., PARK, W., KIM, H.-J., AND KOH, H.-M., Simulation Based Probability Model of Impact Load Due to Ship-bridge Collision, Proceedings of the IABSE 2012 Conference, 8, pp. 19-26, Sharm El Sheikh, Egypt, 2012.
21. IWAI, A. AND SHOJI, K., On the Effect of Wind around the Pier upon the course-keeping of Ship, *Publication of Japan Institute of Navigation*, 11, pp.15-21, 1978.
22. IWAI, A., NAGASAWA, H., ODA, K. AND SHOJI, K., Ship-bridge-pier Protective System, *Coastal Engineering*, 136, pp. 2261-2276, 1980.
23. MONTEWKA, J., Analytical and Simulation Methods for Determine Vessel's Safety Maneuvering area – Usefulness Assessment, *Proceedings of the XVI-th International Science and Technology Conference*, Gdynia, Poland. 2008.
24. TSENG, M.-H., YEN, C.-L. AND SONG, C.C.S., Computation of Three-dimensional Flow around Square and Circular Piers, *International Journal for Numerical Methods in Fluids*, 34, pp.207-227, 2000.
25. SALAHELDIN, T. M., IMRAN, J. AND CHAUDHRY, M. H., Numerical Modeling of Three-dimensional Flow Field around Circular Piers, *Journal of Hydraulic Engineering*, 130(2), pp.91–100, 2004.
26. MINORSKY, V.U., An Analysis of Ship Collision with Reference to Protection of Nuclear Power Plants, *Journal of Ship Research*, 3, pp. 1-4, 1959.
27. BREUSERS, H.N.C., AND RAUDKIVI, A.J., *Scouring*, Rotterdam: Balkema, 1991.
28. GRAF, W.H., AND ALTINAKAR, M.S., Experiments on Flow around a Cylinder; the Velocity and Vorticity fields, *Journal of Hydraulic Research*, 36(4), pp. 637-653, 1998.